Proceedings of 10th International Conference on Precision, Meso, Micro and Nano Engineering (COPEN 10)
December 07 – 09, 2017, Indian Institute of Technology Madras, Chennai – 600 036 INDIA

Numerical Study of Constrained Groove Pressing to Produce Nano-structured Metallic Materials

Sunil Kumar[a], K Hariharan[b] and D Ravi Kumar[a]

[a] Department of Mechanical Engineering, Indian Institute of Technology, Delhi - 110016, INDIA
[b] Department of Mechanical Engineering, Indian Institute of Technology, Chennai - 600036, INDIA

Abstract

Constrained groove pressing (CGP) is one of the severe plastic deformation (SPD) techniques to produce ultra-fine grained sheet metals. A typical CGP process include four stages of groove pressing and flattening. In the present work, finite element analysis of CGP process is performed for one complete pass to simulate all the four stages. The homogeneity and evolution of the stress and strain distribution in the plane of the sheet are analyzed in each stage. It is observed that the central region exhibits higher strain hardening when compared to the corners due to the additional bending in the corner region. The finite element results are validated using the experimental data of commercially pure aluminum and low carbon steel published in literature.

Keywords:Severe Plastic Deformation, Constrained Groove Pressing, Finite Element Analysis, CommerciallyPure Aluminum and Low Carbon Steel.

1. INTRODUCTION

Severe Plastic Deformation (SPD) methods are used to produce ultrafine grained (UFG) materials with superior mechanical properties. Among the different SPD techniques, repetitive corrugation and straightening (RCS)[1], constrained grooving and pressing (CGP)[2] and accumulative roll bonding (ARB)[3]are commonly utilized for sheet or plate metals. In CGP technique, grain refinement is achieved by repeated shear deformation through asymmetric groove and flat dies under plain strain condition. Each CGP pass consists of four stages; two corrugated groove pressing stages alternated with two flattening stages. An equivalent plastic strain of 1.16 is induced in each pass for 45^0 groove angle as in equation (1). The degree of grain refinement increases with the number of passes. The amount of plastic strain is dependent on the number of passes and die geometry such as groove angle under the plane strain shear deformation using the equation (1) of effective strain.

$$\varepsilon_{eff} = 2n\frac{\gamma}{\sqrt{3}} = 2n\frac{\tan\theta}{\sqrt{3}} \quad (1)$$

Where, n is the number of passes and θ is the groove angle

The plastic strain induced is highly non-homogenous leading to non-uniform refinement of grains in the material[4]. It is therefore important to analyze the strain inhomogeneity during CGP process. The strain inhomogeneity in this CGP process is significantly influenced by the geometric parameters (die angle, width of flat region, and corner radius of grooved dies) and material properties (strain hardening coefficient and strain hardening exponent). The past studies have focused on the effect of die design, and the deformation modes in different regions affecting the strain inhomogeneity [4-8]. Most of the studies have simulated only the first two stages of CGP and the strain distribution in subsequent stages have not been studied in detail. In addition to the above, the relative contribution of different materials for a given set of parameters has not received attention in the past.

In this paper, we have considered two different materials, low carbon steel and commercially purealuminum for processing through CGP. The objective of the work is to numerically analyze the CGP process for these two materials and estimate the strain inhomogeneity.Homogenous strain distribution will lead to uniform grain refinement. The outcome of the present study will be used to understand the effectiveness of CGP processing route to produce UFG in different base metals.

2. FINITE ELEMENT SIMULATION

Finite element simulation of CGP process was carried out using commercial ABAQUS/Standard software. Owing to the symmetry, only a section of the sample (28X2 mm^2) was analyzed under plain strain condition. Isotropic material properties was assumed to analyze the CGP pressing. For both materials, the properties are tabulated in Table 1and theinput stress strain curve($K\sigma^n$)for simulation is shown in Fig.1. All the four stages of one CGP pass is simulated. Grooved and flattened dies were considered as analytical rigid bodies with 45^0 groove angle and 2mm groove width. The material deformation was studied at room temperature and was assumed to be strain rate independent. Therefore, the stress and strain results in the material are independent of tool velocity in the simulation. A relative high tool velocity was used in the simulation. Displacement based constraints were used to define the tool motion. Sheet was modelled as a deformable part and meshed using CPE4R (Bilinear plane strain quadrilateral, reduced integration, hourglass control) element type with a total of 2048 elements. The tools were modelled as analytically rigid parts.The coefficient of friction between sheet and die surface interface was assumed as 0.1 throughout the analysis.

3. RESULTS AND DISCUSSION

3.1. Material deformation behavior

Fig.2 illustrates the variation of equivalent plastic strainand material behavior of low carbon steel and aluminum at different stages. Theoretically a uniform distribution of value 1.16 was expected at the end of one pass. It can be seen however that the strain distribution is non-uniform. This will result in non-uniform grain refinement as the refinement is dependent upon dislocation accumulation through plastic strain. In general the following observations are made on both the materials.

After first stage, alternate slant regions of grooves are subjected to shear deformation. Expected shear strain of 0.58 is not observed in these alternate deformed regions. The maximum strain for low carbon steel and aluminum are about 0.87 and 0.88 respectively. Maximum strain values occur at the middle of slant region and decreases towards the corners. Non-uniformity of strain is due to bending at the corners which cause additional deformation in flat region. In the 2nd stage, sheet is

ISBN: 978-93-80689-28-9

flattened by reverse shearing and bending as it is in 1st stage in forward direction. Equivalent plastic strain for both the materials is 1.6 after 2nd stage which is far from theoretical value. Similar observations of 1st and 2nd stages of deformed regions are found in 3rd and 4th stages. Since the un-deformed material is slightly hardened after 2nd stage flattening, material has received higher strain in 4th stage flattening. After 4th stage, maximum equivalent plastic strains for low carbon steel and aluminum are 1.76 and 1.69 respectively along center line as shown in Fig. 3, which is significantly higher than the theoretical value. Strain distribution contours of both materials are similar.

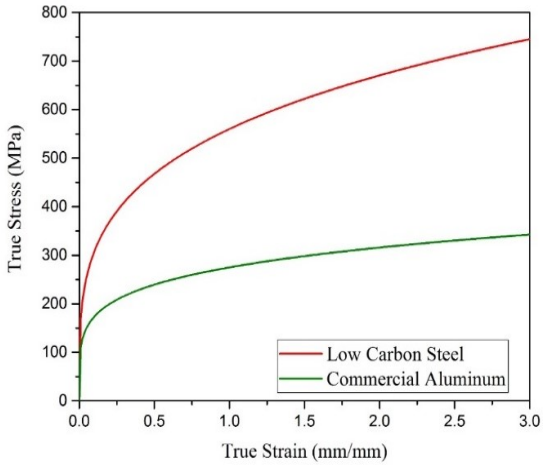

Fig.1- Stress-strain curve incorporated in finite element simulation

Table 1 Material properties incorporated in finite element simulation

Materials Selected→ Material Properties↓	Low Carbon Steel	Aluminum
Strain Hardening Exponent 'n'	0.26	0.2
Strain Hardening Coefficient 'K' (MPa)	560	275
Density (Kg/mm^3)	7870	2710
Young Modulus (GPa)	200	70
Poison Ratio	0.3	0.33
Yield Strength (MPa)	225	116
Ultimate Tensile Strength(MPa)	300	148

3.2. Strain and Stress Distribution

Fig. 3 and Fig. 4 represent the effective strain and stress distribution at the central line of the both deformed material respectively. Plastic strains vary harmonically along the transverse direction and are symmetrically distributed after each groove. Strain distribution shows peaks of maximum strain at the middle of groove region and valleys of minimum strain at the corner region. According to die geometry, sheet at 2mm distance from both the ends are not subjected to any shear deformation, but sheet shows some deformations in these region too. This is due to the corner effect mentioned in the previous section. Analyzing the strain distribution, it is found that strain peaks are observed in 4th stage flattening is slightly more compare to peaks of 2nd stage flattening due to work hardening of materials in previous stages. The same trend of effective strain distribution in finite element simulation of CGP process is also observed in other research [4,9,8].

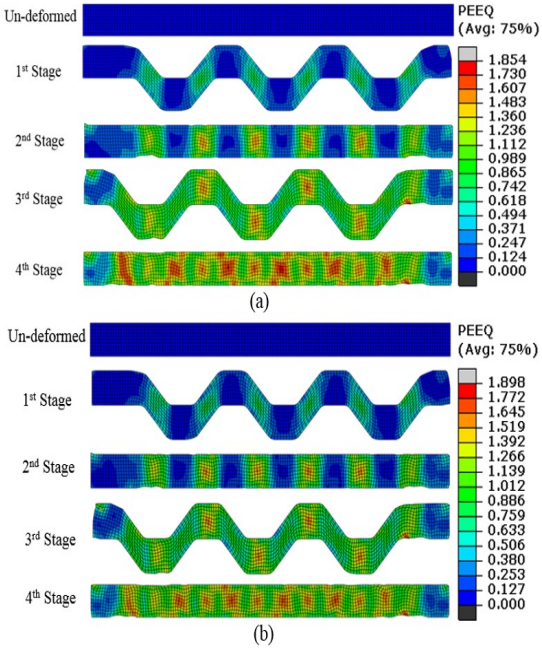

Fig.2-Equivalent plastic strain distribution contours (a) low carbon steel (b) aluminum.

As indicated earlier, inhomogeneity of strain distribution results in non-uniformity of ultrafine grains and mechanical properties. Inhomogeneity factor (IF) as in equation (2) is used to quantify the non-uniformity in strain distribution.

$$IF = \frac{\sqrt{\sum_{i=1}^{n} \frac{(S_i - S_{avg})^2}{n-1}}}{S_{avg}} \times 100 \quad (2)$$

Where, S_i= strain value at ith point, S_{avg} = average strain value, n=number of measurements in single sample

Larger the IF value more significant is the inhomogeneity in material properties. After 1st pass, IF values for low carbon steel and aluminum are 24.7 and 25.2 respectively indicating slightly higher IF foraluminum. Since low carbon steel has lower IF value, it may be inferredthat it has higher uniformity in grain refinement and mechanical properties.

Aluminum shows more uniformity in equivalent stress distribution compared to low carbon steel along center line as shown in Fig. 4. This is due to low stress gradient at large strain and low strain hardening exponent (n) of aluminum in comparison to low carbon steel [10].

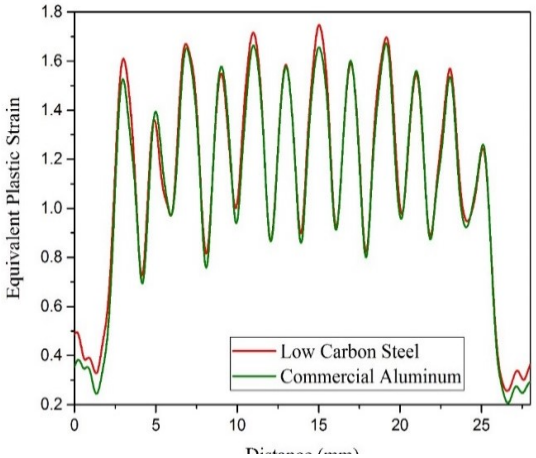

Fig.3-Plastic strain distributions along center line after 4th stage

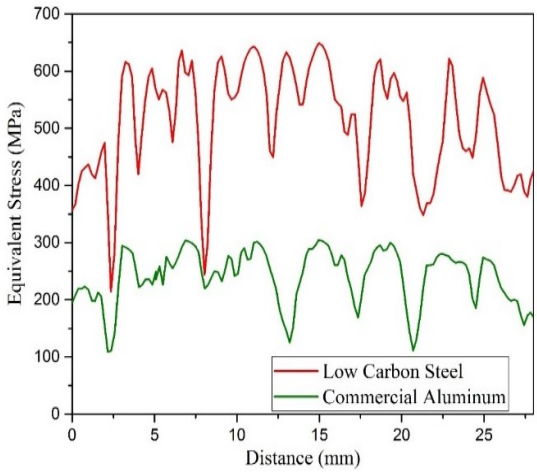

Fig.4-Equivalent stress distributions along center line after 4th stage

Although the strain distribution of both the materials are almost similar, their stress distribution is distinctly different. This is due to the values of strength coefficient 'K' and strain hardening exponent 'n' in stress strain constitutive relation. The peak stress of aluminum is much lower than low carbon steel. Also, the variation of stress across the corner in aluminum is less steep when compared to the low carbon steel. This is due to the low value of 'n' in Al when compared to steel. One can conclude on the bases of selected two materials study in current geometry that material should have large 'n' for high peak strains and uniform strain distribution, whereas lower 'n' value for uniform stress distribution at strains. Large 'n' leads to more grain refinement and uniform strengthening of the material. Uniform grain structure produces less non-homogenous microstructure and mechanical properties which is essential for commercial use by increasing the formability of the sheet.

3.3. Load Estimation

Fig. 5 represents the load-stroke curve from simulation of 1st and 2nd stages of two materials. Since 3rd and 4th stages are repetitions of 1st and 2nd stage, the related curves are not mentioned here. The load-stroke curves are similar to the load-punch travel curve in V- or U- die bending and closed die forging operation. All curves are characterized in three phases. In the first phase, the steep curve indicates instant load requirement for bending. Further, load is almost constant in all the cases due to shearing of material. At the end of the stroke, the significant increase in load shows that material is subjected to bottoming. In both the materials, load requirement in flattening operation is more because the material is already strain hardened during grooving operation. Maximum load values from simulation of CGP using low carbon steel and aluminum are 27.5kN and 12.8kN respectively. In CGP processing, the total load is the contribution of the load required from bending, shearing, and stretching of slant regions.Similar kind of load-stroke curves were also observed in previously published literature [4,6,8].

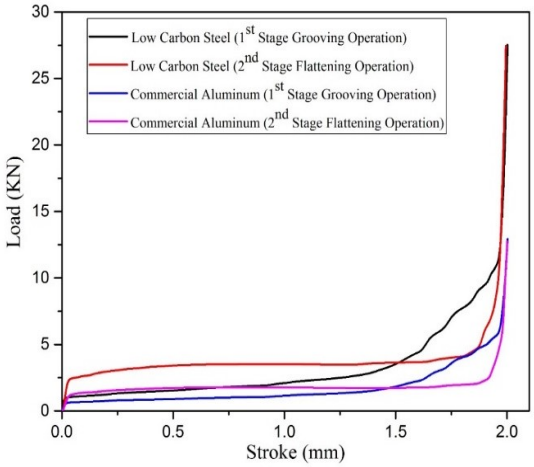

Fig. 5-Load–stroke curves predicted by finite element simulation

4. CONCLUSIONS

1) The effect of different materials on the mechanics of CGP process is analyzed using low carbon steel and commercially pure aluminum. It was found that the inhomogeneous strain distribution is highly influenced by the strain hardening exponent. Since the degree of grain refinement is related to the uniformity of plastic strain distribution, the materials with high 'n' will yield better results in CGP.
2) It was found that the constrained groove pressing process involves additional bending instead of shear deformation near the corners that decreases the peak strain and also serves as a source of non-uniform distribution.
3) The maximum load estimated from simulation of CGP using low carbon steel and aluminum are 27.5KN and 12.8KN respectively. In CGP processing, the total load is the contribution of the load required from bending, shearing, and stretching of slant regions.

References

[1] J.Y. Huang, Y.T. Zhu, H. Jiang, T.C. Lowe, Microstructures and dislocation configurations in nanostructured Cu processed by repetitive corrugation and straightening, Acta Mater. **49** (2001) 1497–1505.

[2] D.H. Shin, J.J. Park, Y.S. Kim, K.T. Park, Constrained groove pressing and its application to grain refinement of aluminum, Mater. Sci. Eng. A. **328** (2002) 98–103.

[3] Y. Saito, H. Utsunomiya, N. Tsuji, T. Sakai, Novel ultra-high straining process for bulk materials—development of the accumulative roll-bonding (ARB) process, Acta Mater. **47** (1999) 579–583.

[4] Z.S. Wang, Y.-J. Guan, G.-C. Wang, C.-K. Zhong, Influences of die structure on constrained groove pressing of commercially pure Ni sheets, J. Mater. Process. Technol. **215** (2015) 205–218.

[5] K. Peng, Y. Zhang, L.L. Shaw, K.W. Qian, Microstructure dependence of a Cu-38Zn alloy on processing conditions of constrained groove pressing, Acta Mater. **57** (2009) 5543–5553.

[6] A. Sajadi, M. Ebrahimi, F. Djavanroodi, Experimental and numerical investigation of Al properties fabricated by CGP process, Mater. Sci. Eng. A. **552** (2012) 97–103.

[7] M. Borhani, F. Djavanroodi, Rubber pad-constrained groove pressing process : Experimental and finite element investigation, Mater. Sci. Eng. A. **546** (2012) 1–7.

[8] S.S. Satheesh Kumar, I. Balasundar, T. Raghu, Finite Element Analysis of Constrained Groove Pressing of Pure Aluminum Sheets, Int. J. Comput. Mater. Sci. Eng. **2** (2013) 1350001.

[9] S.C. Yoon, A. Krishnaiah, U. Chakkingal, H.S. Kim, Severe plastic deformation and strain localization in groove pressing, Comput. Mater. Sci. **43** (2008) 641–645.

[10] S.C. Yoon, P. Quang, S.I. Hong, H.S. Kim, Die design for homogeneous plastic deformation during equal channel angular pressing, J. Mater. Process. Technol. **187** (2007) 46–50.